



Afdelingen for Bærende Konstruktioner  
Department of Structural Engineering  
Danmarks Tekniske Højskole · Technical University of Denmark

## Arch Effect in Reinforced Concrete one-way Slabs

Bent Steen Andreasen

M.P. Nielsen

Serie R

No 275

1991

ARCH EFFECT IN  
REINFORCED CONCRETE  
ONE-WAY SLABS

Bent Steen Andreasen \*

M.P. Nielsen \*\*

\* Civilingeniør, stud.lic., Afdelingen for Bærende Konstruktioner,  
Danmarks tekniske Højskole.

\*\* Professor, dr.techn., Afdelingen for Bærende Konstruktioner,  
Danmarks tekniske Højskole.

**Arch Effect in Reinforced Concrete one-way Slabs**

Copyright © by Bent Steen Andreasen, M.P. Nielsen, 1991

Tryk:

Afdelingen for Bærende Konstruktioner

Danmarks Tekniske Højskole

Lyngby

ISBN 87-7740-077-1

SYNOPSIS

It is well known that the load carrying capacity of reinforced concrete slabs with horizontal restraints can be several times that found by the yield line theory.

The way in which the theory of perfectly plastic materials can be used to derive expressions for the load carrying capacity for reinforced concrete slab strips with horizontal restraints at the edges will be demonstrated here.

For slab strips, the deflection at maximum load is a very important parameter. A simple expression for the deflection as a function of the slenderness of the slab is derived.

The theory is compared with test results and the agreement is found to be satisfactory.

1. NOTATIONS

|              |   |
|--------------|---|
| a            | Distance from support to load or half the slab length.                          |
| b            | Width of slab strip.  |
| d            | Effective depth for the bottom reinforcement.                                   |
| d'           | Effective depth for the top reinforcement.                                      |
| $f_c$        | Uniaxial compressive strength of concrete (measured on 150 x 300 mm cylinders). |
| $f_y$        | Yield strength of reinforcement.  |
| h            | Depth of slab.  |
| $k_l$        | Load factor.  |
| l            | Slab length.  |
| m            | Dimensionless moment.   |
| $m_J$        | Moment, $m_J = m h^2 f_c$ .   |
| $m_m$        | Dimensionless membrane moment.  |
| $m_M$        | Membrane moment $m_M = m_m h^2 f_c$ .   |
| $m_n$        | Dimensionless moment of reduction.  |
| p            | Uniform load.   |
| $\bar{p}$    | Line load.  |
| $\dot{w}$    | Increment of the deflection.  |
| w            | Deflection at mid-span.   |
| $A_s$        | Cross-sectional area of the bottom reinforcement.                               |
| $A'_s$       | Cross-sectional area of the top reinforcement.                                  |
| H            | Horizontal force.   |
| P            | Total load on slab.   |
| $P_{test}$   | Total load obtained in test.  |
| $P_{theory}$ | Total theoretical load carrying capacity.                                       |
| $P_J$        | Total load carrying capacity, according to the yield line theory.               |
| $P_M$        | Total membrane load carrying capacity.  |
| $P_N$        | Total reduction in the load carrying capacity.                                  |
| $W_e$        | External work.  |
| $W_i$        | Internal work.  |
| $\alpha$     | The ratio between the bottom reinforcement in compression and that in tension.  |
| $\beta$      | The ratio between the top reinforcement in compression and that in tension.     |

- $\gamma$  Relative effective depth for the bottom reinforcement,  $\gamma = d/h$  .
- $\gamma'$  Relative effective depth for the top reinforcement,  $\gamma' = d'/h$  .
- $\delta$  Relative deflection at mid-span,  $\delta = w/h$  .
- $\lambda$  Slenderness of slab  $\lambda = l/h$  .
- $\nu$  Effectiveness factor.
- $\xi$  Compressive zone relative to the depth  $h$  .
- $\phi$  Mechanical degree of bottom reinforcement  $\phi = \frac{A_s f_y}{h f_c}$  .
- $\phi'$  Mechanical degree of top reinforcement  $\phi' = \frac{A'_s f_y}{h f_c}$  .

## 2. INTRODUCTION

In normal first-order calculations based on the theory of plasticity, the changes in geometry are not taken into account. As is known, this normally gives good results when comparing theory with test results. Since slabs are often flexible structures, the changes in geometry sometimes have a considerable effect on the load carrying capacity. This is known as the membrane effect. For small deflections, the compressive membrane effect predominates, and for larger deflections, it is the tensile membrane effect which predominates. In a simply supported slab, only tensile membrane action is normally considered, but in a slab with horizontal restraints along the edges, depending on the size of the deflection, both compressive and tensile membrane actions may be present.

A simple explanation of the compressive membrane action is presented here. In pure bending of reinforced concrete with small steel ratios, the neutral axis is at failure, very close to the compressive surface of the concrete. This means that pure bending is accompanied by extensions of the centroid. If the support conditions are such, that these deformations cannot take place (horizontal restraints), failure corresponding to pure bending cannot occur. The neutral axis must be forced down towards the centroid of the section, which requires that large compressive membrane forces must be supplied by the support. The compression zones in this case are of the order of half the slab thickness, and the ultimate moment, and therefore the total load is very high.

A slab strip, having horizontal restraints along the supports, typically has a load carrying capacity, which is from 3 to 6 times the normal yield line strength. If the ultimate strength due to membrane action could be taken into account in a simple way, it would be possible to utilize these large reserves. Expressions for the total load carrying capacity of a slab strip with horizontal restraints along the supported edges will be attempted to be found in this paper.

### 3. BASIC ASSUMPTIONS

The theory of plasticity is applied. In the calculations, the lower and the upper bound theorems are used to develop expressions for the ultimate load carrying capacity. In the upper bound calculations, the yield line concept for plane stress is used to find the dissipation.

The concrete is assumed to be a rigid, plastic material. Coulomb's failure criterion, together with a limitation of the tensile strength, the modified Coulomb failure criterion, is used as yield condition. The tensile strength is considered to be zero.

The well known fact that concrete is not perfectly plastic is taken into account by reducing the uniaxial compressive strength  $f_c$  by the effectiveness factor  $\nu$ . The effective plastic strength is then taken to be  $f_{cp} = \nu f_c$ .

The reinforcement is assumed to be rigid-plastic and to carry only longitudinal stresses. Thus, dowel effects are not taken into account.

### 4. THEORETICAL LOAD CARRYING CAPACITY

The load carrying capacity of a slab strip with horizontal restraints along the supported edges is found by using both the lower and upper bound theorems.

In connection with the lower bound calculations, the concept of "membrane moment" is defined.

#### 4.1 Lower bound solution

A plain concrete slab strip with a line load and horizontal restraints at the edges is considered, see figure 4.1.1.



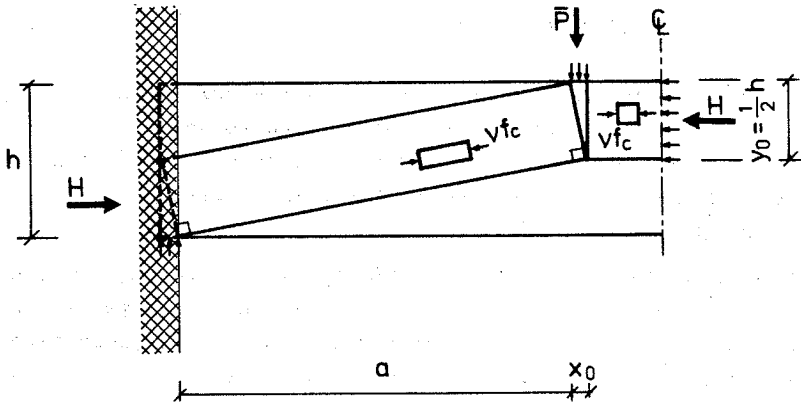


Figure 4.1.1: Slab strip with horizontal restraints and loaded with a line load. The deflection is zero.

A lower bound solution in this case can be found to be

$$\bar{p} = v f_c x_0 = v f_c \cdot \frac{1}{2} a \left[ \sqrt{1 + \left(\frac{h}{a}\right)^2} - 1 \right] \quad (4.1.1)$$

where the geometrical parameters  $x_0$ ,  $a$  and  $h$  are shown in figure 4.1.1. The same solution is found for beams without shear reinforcement, see Nielsen [84.1].

For  $h/a \ll 1$ , (4.1.1) can, with good approximation, be written as

$$\bar{p} = \frac{1}{a} \cdot \frac{1}{4} v f_c h^2 \quad (4.1.2)$$

If the width of the slab strip is  $b$ , (4.1.2) can be rewritten as

$$P = \bar{p}b = \frac{b}{a} \cdot \frac{1}{4} v f_c h^2 \quad (4.1.3)$$

(4.1.3) is based on the assumption that the deflection  $w$  under the line load of the slab is zero. If the deflection is other than zero, the load carrying capacity can be found by replacing  $h$  by

the effective depth  $(1-\delta)h$ , where  $\delta = w/h$  is the relative deflection under the line load, see figure 4.1.2.

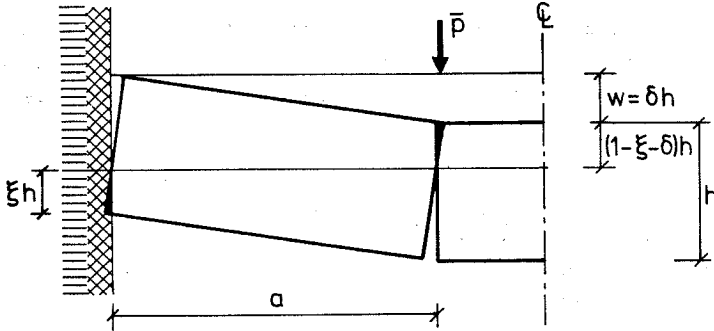


Figure 4.1.2: Slab strip with the deflection  $w = \delta h$  under the line load.

The expression for the load carrying capacity as a function of the deflection  $\delta = w/h$ , is then found to be

$$P = \bar{p}b = \frac{b}{a} \cdot \frac{1}{4} \nu f_c h^2 (1 - \delta)^2 \quad (4.1.4)$$

Introducing the membrane moment,  $m_M$ , as

$$m_M = \frac{1}{4} \nu f_c h^2 (1 - \delta)^2 \quad (4.1.5)$$

the expression for the total load carrying capacity (4.1.4) can be written as

$$P = \frac{b}{a} \cdot m_M \quad (4.1.6)$$

The expression for the membrane moment (4.1.5) can be rewritten as

$$m_M = \left(\frac{1}{2}h(1-\delta)\right) v f_c \cdot \left(\frac{1}{2}h(1-\delta)\right) \quad (4.1.7)$$

It can be seen that stresses in two cross sections give rise to the membrane moment. The compression zones have a depth of  $\frac{1}{2}h(1-\delta)$  and the distance between the resultant forces is  $\frac{1}{2}h(1-\delta)$ .

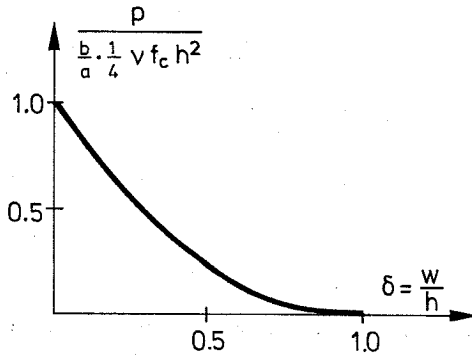


Figure 4.1.3: The load carrying capacity for a plain concrete slab strip with horizontal restraints at the edges, as a function of the relative displacement under the line load.

In figure 4.1.3 the load carrying capacity (4.1.6) is given as a function of the relative displacement  $\delta$ . The load carrying capacity approaches zero, when the relative displacement,  $\delta$ , approaches one. This is because the effective depth of the cross section approaches zero, whereby a compression arch cannot be established.

#### 4.2 Upper bound solution

A slab strip similar to that in the previous section is considered, but now it is assumed that the slab is reinforced with tension and

compression reinforcement , see figure 4.2.1.

The load is assumed to be symmetrical about the centre line of the slab, but otherwise arbitrary. A failure mechanism with yield lines along both edges and along the centre line is considered.

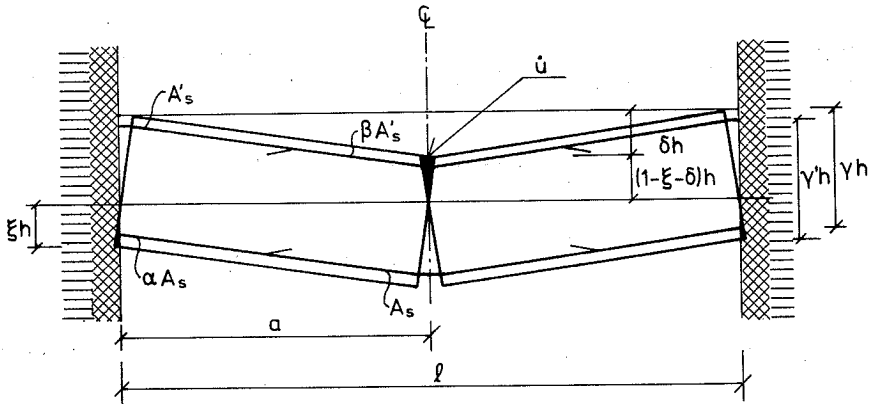


Figure 4.2.1: Slab strip with a deflection  $w = \delta h$  in the middle and tension and compression reinforcement.

Giving the deformed slab, shown in figure 4.2.1, an incremental deflection,  $\dot{w}$ , at mid-span the internal work dissipated in the structure can be written as

$$W_i = 2 b h^2 f_c \cdot \frac{\dot{w}}{a} \left[ \frac{1}{2} v \left( (1 - \xi - \delta)^2 + \xi^2 \right) + (\gamma - 1 + \xi + \delta) \phi + (\gamma' - \xi) \phi' + (\gamma - 1 + \xi) \alpha \phi + (\gamma' - \xi - \delta) \beta \phi' \right] \quad (4.2.1)$$

The symbols used, can be found in figure 4.2.1, where it is assumed that the reinforcements,  $\alpha \phi$  and  $\beta \phi'$  are always in compression zones.

By minimizing the internal work with respect to the relative depth of

the compression zone  $\xi$ , the optimal value for  $\xi$  is found to be

$$\xi = \frac{1}{2}(1 - \delta - \frac{1}{v}((1 + \alpha)\phi - (1 + \beta)\phi')) \quad (4.2.2)$$

Inserting (4.2.2) into (4.2.1), the internal work can be written as

$$\begin{aligned} W_i = 2bh^2 f_c \frac{\dot{w}}{a} & \left[ (1 + \alpha)\phi\left(\gamma - \frac{1 + \alpha}{2v}\phi\right) + (1 + \beta)\phi'\left(\gamma' - \frac{1 + \beta}{2v}\phi'\right) \right. \\ & - \frac{1}{2}(1 + \alpha)\phi\left(1 - \frac{1 + \alpha}{2v}\phi\right) - \frac{1}{2}(1 + \beta)\phi'\left(1 - \frac{1 + \beta}{2v}\phi'\right) \\ & + \frac{1}{2}\delta((1 - \alpha)\phi + (1 - \beta)\phi') + \frac{1}{2v}(1 + \alpha)(1 + \beta)\phi\phi' \\ & \left. + \frac{v}{4}(1 - \delta)^2 \right] \quad (4.2.3) \end{aligned}$$

Defining  $m$ ,  $m_n$  and  $m_m$  as

$$\begin{aligned} m = \phi\left(\gamma - \frac{\phi}{2v}\right) + \alpha\phi\left(\gamma - \frac{\alpha\phi}{2v}\right) + \phi'\left(\gamma' - \frac{\phi'}{2v}\right) + \beta\phi'\left(\gamma' - \frac{\beta\phi'}{2v}\right) \\ + \frac{1}{v}(\alpha + \beta)\phi\phi' - (\alpha\phi + \beta\phi') \quad (4.2.4) \end{aligned}$$

$$\begin{aligned} m_n = \frac{1}{2v}(1 + \alpha)(1 + \beta)\phi\phi' + \frac{1}{2}\delta((1 - \alpha)\phi + (1 - \beta)\phi') \\ - \frac{1}{2}(1 + \alpha)\phi\left(1 - \frac{(1 + \alpha)\phi}{2v}\right) - \frac{1}{2}(1 + \beta)\phi'\left(1 - \frac{(1 + \beta)\phi'}{2v}\right) \\ + \alpha\phi\left(1 - \frac{\phi}{v}\right) + \beta\phi'\left(1 - \frac{\phi'}{v}\right) \quad (4.2.5) \end{aligned}$$

$$m_m = \frac{v}{4}(1 - \delta)^2 \quad (4.2.6)$$

(4.2.3) can be transformed into the more compact form.

$$W_i = 2 b h^2 f_c \cdot \frac{\dot{w}}{a} [m + m_n + m_m] \quad (4.2.7)$$

As can be seen from (4.2.4),  $m$  is the normal bending yield moment and, as in the previous section,  $m_m$  represents the membrane moment, according to (4.1.5).  $m_n$  can be interpreted as a reduction, caused by the combined bending and membrane actions.

The external work is

$$W_e = \frac{4}{k_\ell} \cdot P \dot{w} \quad (4.2.8)$$

where the load factor  $k_\ell$  is shown in figure 4.2.2 for some common arrangements of loading.

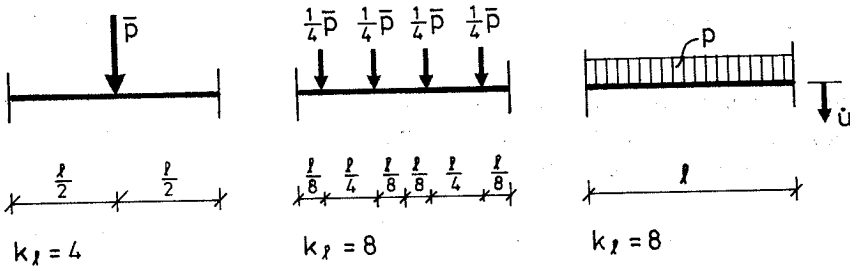


Figure 4.2.2: Examples of load factor  $k_\ell$  for different arrangements of loading.

Using the upper bound theorem, the expression for the total load carrying capacity can be written as

$$\frac{P}{h^2 f_c} = k_\ell \frac{b}{\ell} [m + m_n + m_m] \quad (4.2.9)$$

(4.2.2)-(4.2.7) and (4.2.9) are only valid when  $\xi \geq 0$ . From this condition, we find, using (4.2.2) that

$$\delta \leq 1 - \frac{1}{v}((1 + \alpha)\phi - (1 + \beta)\phi') \quad (4.2.10)$$

Minimizing (4.2.9) with respect to  $\delta$ , and inserting  $\alpha = \beta = 0$  for simplicity, we find

$$\delta = 1 - \frac{1}{v}(\phi + \phi') \quad (4.2.11)$$

which corresponds to the minimum value for the load-deflection relationship.

Inserting (4.2.11) into (4.2.5) and (4.2.6),  $m$  and  $m_n$  are given by

$$m_m = -m_n = \frac{1}{4v}(\phi + \phi')^2 \quad (4.2.12)$$

The only term left in the expression (4.2.9) is  $m$ . Using  $\delta$  determined from (4.2.11), the depth of the compression zones at mid-span and at the edges are found to be

$$(1 - \xi - \delta)h = \frac{\phi}{v}h, \quad \xi h = \frac{\phi'}{v}h. \quad (4.2.13)$$

This corresponds to pure bending in the middle and the edge sections, respectively. Therefore this is the same solution as obtained by a normal yield line calculation.

The load carrying capacity, (4.2.9), is shown as a function of the relative deflection,  $\delta$ , for some cases in figures 4.2.3 and 4.2.4.

The solution shown, can also be found by using a three dimensional method introduced by Calladine [68.1]. The three dimensional method is used in Andreasen [85.1] and Andreasen & Nielsen [86.1].

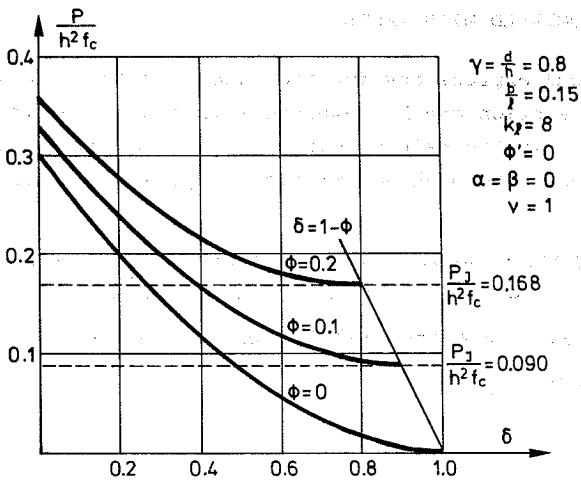


Figure 4.2.3: The load carrying capacity as a function of the relative deflection  $\delta$ . Curves for different values of  $\phi$ .

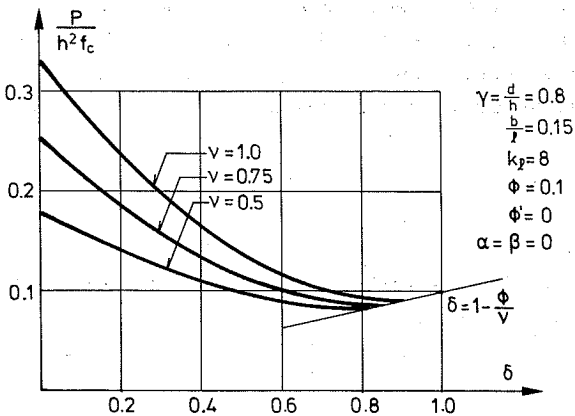


Figure 4.2.4: The load carrying capacity as a function of the relative deflection  $\delta$ . Curves for different values of  $\nu$ .



## 5. THEORY COMPARED WITH TESTS

The theoretical expressions for the load carrying capacity from the previous section can be compared with results of tests on slap strips. Only the main results of this analysis will be given here. A more thorough description is given in Andreasen [85.1].

The tests are reported in Roberts [69.1] and Birke [75.1]. From Birke only test series 2 is included in the analysis.

The load carrying capacity (4.2.9) can be written as

$$P = P_J + P_N + P_M \quad (5.1)$$

where

$$\frac{P_J}{h^2 f_c} = k_\ell \frac{b}{\ell} m, \quad \frac{P_N}{h^2 f_c} = k_\ell \frac{b}{\ell} m_n, \quad \frac{P_M}{h^2 f_c} = k_\ell \frac{b}{\ell} m_m \quad (5.2)$$

The load carrying capacity obtained in the tests,  $P_{\text{test}}$ , is compared with  $P$  in (5.1). The mean value and the standard deviation of the ratio test/theory were about 1.00 and 0.11, respectively. To calculate  $P_{\text{theory}}$ , the relative deflection obtained in each test was used. The effectiveness factor,  $\nu$ , as a function of the uniaxial compressive cylindrical strength  $f_c$  was taken to be

$$\nu = \frac{4.88}{\sqrt{f_c}} + 0.16 \quad (f_c \text{ in MPa}) \quad (5.3)$$

The 58 tests (36 from Roberts and 22 from Birke), covered the following range of parameters:

- $f_c$  between 14 and 45 MPa
- $\phi$  between 0 and 0,192
- $\delta$  between 0,08 and 0,31
- $\lambda$  between 10 and 29
- $\alpha = \beta = \phi' = 0$

As the theoretical expression is complicated, an attempt to simplify it has been made. Expression (5.1) is modified as

$$P = P_J + P_M \quad (5.4)$$

where (5.2) still is valid.

In (5.4) the term which takes into account the combined bending and membrane actions, is disregarded. Thus the effectiveness factor  $\nu$  must be reduced, compared to the value in the theoretically correct analysis.  $P_N$  is therefore included in the reduced  $\nu$  value. When comparing (5.4) with the test results, the reduced value  $\nu$  can be calculated from

$$\nu = \frac{4.39}{\sqrt{f_c}} + 0.14 \quad (f_c \text{ in MPa}) \quad (5.5)$$

(5.5) is identical with expression (5.3), multiplied by 0.9.

Using (5.4) as the theoretical load carrying capacity, where  $\nu$  is determined from (5.5), the mean and the standard deviations of the ratio test/theory were 1.01 and 0.14, respectively. The results from the two analyses are almost identical.

Christiansen & Frederiksen, [83.1] and [83.2], showed by means of an empirical analysis that the load carrying capacity of slabs horizontally restrained along the edges could be found by an expression similar to (5.4). The contribution from the membrane action,  $P_M$ , is, in their expression, a constant multiplied by  $h^2 f_c$ . The constant depends on the degree of horizontal restraint.

From expression (4.2.6), it can be seen that the membrane moment  $m_m$  amongst other things, depends on the relative deflection  $\delta$ . As  $m_m$  is a function of  $(1-\delta)^2$ , a change in  $\delta$  results in a relatively large change in  $m_m$ , when  $\delta$  lies between 0 and 0.5. Since the deflection of slab strips at maximum load normally lies within that interval, it is important, that the deflection can be determined very accurately. This problem is dealt with in the next section.

## 6. THE RELATIVE DEFLECTION

The relative deflection,  $\delta$ , is, as we have just seen, a very important parameter for determining the membrane moment. In this section a simple method for determining  $\delta$  will be shown.

The slabs are divided into two groups: one group having "rigid" horizontal restraints and the other group having "normal" horizontal restraints. A "rigid" restraint is a restraint which prevents any horizontal displacement at the edges, and a "normal" restraint is a restraint which does not prevent horizontal displacements, but still offers resistance to the vertical displacement. A slab with normal restraint is comparable to slabs built in normal practice. The slabs having rigid horizontal restraints are dealt with first.

Many of the tests from Roberts [69.1] and Birke [75.1] analysed in the previous section, had rigid horizontal restraints. For these tests and for test series 1 from Birke, the relative deflection  $\delta$ , as a function of the slenderness ratio  $\lambda = l/h$  is shown in figure 6.1.

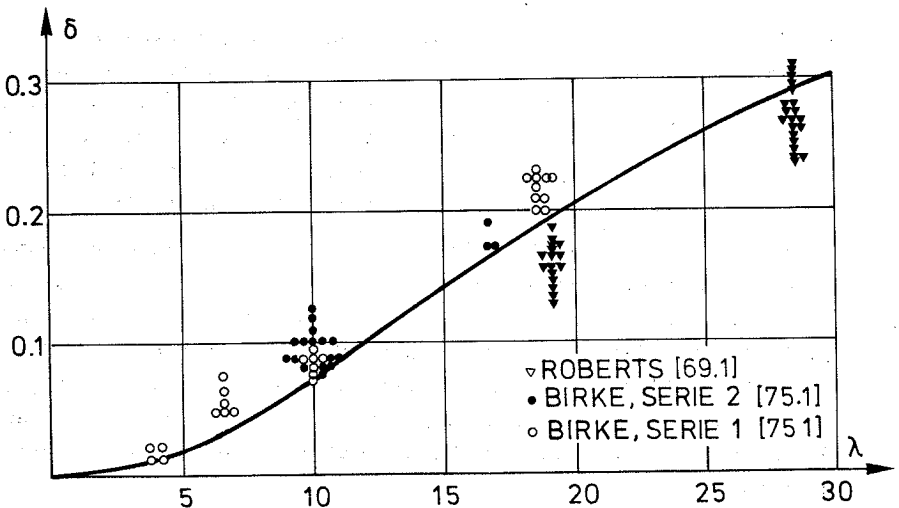


Figure 6.1: The relative deflection as a function of the slenderness ratio for tests with rigid horizontal restraints. The curve shown, is derived from (6.8), inserting  $\rho = 0.0035$ .

Besides the test results, a theoretical curve is shown in figure 6.1. The derivation of this curve is presented in the following. The slab strip is assumed to be deformed, as shown in figure 6.2.

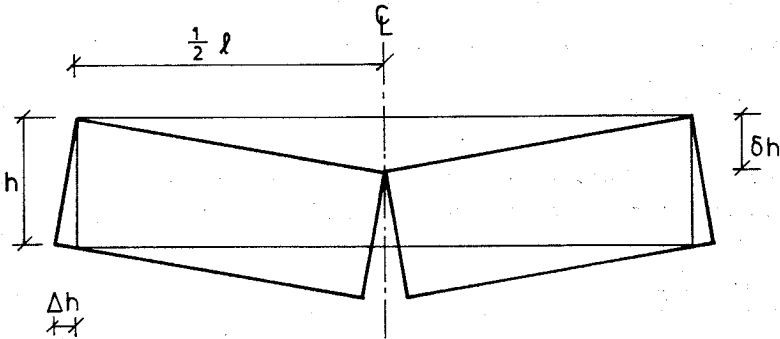


Figure 6.2: Slab part with deflection  $\delta h$  in the middle and a horizontal displacement  $\Delta h$  at the edges.

The relationship between the horizontal displacement,  $\Delta h$ , and the vertical deflection,  $\delta h$ , is found to be

$$\Delta h = 2 \frac{h}{l} \cdot \delta h = \frac{2}{\lambda} \cdot \delta h \quad (6.1)$$

If the slab has a rigid restraint, this displacement can not take place. The horizontal displacement is therefore taken as a deformation inside the slab. The internal horizontal deflection,  $\Delta_1 h$ , for half the slab can be determined by

$$\Delta_1 h = \frac{1}{2} l \cdot \frac{H}{EA} \quad (6.2)$$

where

H is the horizontal force (per unit length)

E is an effective modulus of elasticity (elastic-plastic)

A is an effective cross-sectional area necessary for carrying the horizontal force.

The horizontal force can be written as

$$H = \xi' h v f_c \quad (6.3)$$

where  $\xi'$  is the relative depth of the compression zone, disregarding the influence of the possible reinforcement.

Inserting (6.3) into (6.2), and using  $A = 1 \cdot h$ , yields

$$\Delta_i h = \frac{v f_c}{2E} \cdot \lambda h \cdot \xi' \quad (6.4)$$

Equating (6.1) and (6.4) the following expression for the relative depth of the compression zone is found

$$\xi' = \frac{2\delta}{\rho \lambda^2} \quad (6.5)$$

where

$$\rho = \frac{v f_c}{2E} \quad (6.6)$$

The internal moment per unit length  $M$  can be written as

$$\frac{M}{v f_c h^2} = \xi' (1 - \xi' - \delta) \quad (6.7)$$

$\xi'$  determined from (6.5) should not be confused with the expressions for  $\xi$  in section 4. The relative compression zone  $\xi$  is determined from the plastic calculations, while  $\xi'$  takes into account the elastic-plastic behaviour.

The value of  $\delta = \delta_0$ , which gives the maximum internal moment, can be found by differentiating  $M$  with respect to  $\delta$ , and making this expression equal to zero. Using this and taking  $\xi'$  from (6.5),  $\delta$  as a function of  $\lambda$  can be found to be

$$\delta = \delta_0 = \frac{\rho \lambda^2}{2\rho \lambda^2 + 4} \quad (6.8)$$

Comparing (6.8) with test results, it is found that  $\rho$  can, with sufficient accuracy, be taken to be a constant equal to 0.0035. Expression (6.8) is, together with test results, shown in figure 6.1 for  $\rho = 0.0035$ .

Birke [75.1] used a similar method to find the moment/deflection relationship, but using his assumptions, it is not possible to find an expression as simple as (6.8) for the relationship between  $\delta$  and  $\lambda$ . The expression (6.8) was developed by Andreassen [85.1] who also dealt with the problem by means of the plastic theory, assuming the concrete to be an elastic-plastic material. This method of solving the problem is similar to the method used by Bråstrup & Morley [80.1] in dealing with circular slabs.

Comparing (6.8) with the more complicated expressions mentioned, it is found that the relationship between  $\delta$  and  $\lambda$  is described with sufficient accuracy by (6.8), see Andreassen [85.1].

For slabs with normal horizontal restraints, the deflection can be calculated by using (6.8) combined with a term which takes into account the displacement at the edges. Hence the total relative deflection can be written as

$$\delta = \delta_o + \delta_s \quad (6.9)$$

where  $\delta_o$  is the deflection from the flexibility of the slab and  $\delta_s$  is the deflection from the horizontal displacement at the edges (flexibility of the supports).  $\delta_s$  can be found by considering figure 6.2 to be

$$\delta_s h = \frac{1}{2} \frac{l}{h} \cdot \Delta_s h \quad (6.10)$$

The horizontal displacement  $\Delta_s h$  can be found by subjecting the supports to the horizontal force from the slab and calculating the deflection for this force. The horizontal force can be determined by

$$H = \xi h \cdot \nu f_c \quad (6.11)$$

where the relative depth of the compression zone,  $\xi$ , can be taken from (4.2.2).  $\Delta_s h$  is then found as a function of  $H$ .

Expressions (6.8) and (6.9) were compared with test results. Instead of using the relative deflection obtained in the tests,

$\delta$  is calculated in the way described. For slabs with rigid, as well as those with normal horizontal restraints, the method is found to be satisfactory.

Comparing the results of tests on slab strips with rigid horizontal restraints by Roberts [69.1] and Birke [75.1], using (6.8) to calculate the relative deflection, the mean and standard deviations of the ratio test/theory were 1.04 and 0.10, respectively, when the theoretical strength was determined by (5.1). Using (5.4) as theoretical strength, the corresponding values obtained were 1.04 and 0.13. As it is seen, the results from these analyses are almost identical to the results obtained from the analysis in section 5, where the relative deflection measured in the individual tests was used.

Expression (6.8) has also been tested on masonry slab strips. The correspondence between test and theory is also here found to be satisfactory, see Yde [87.1] or Nielsen & Yde [87.2].

A similar principle to that shown in (6.9) has been used by Christiansen [63.1], but his final expressions are rather complicated.

#### 7. LOAD-DEFLECTION CURVE: THEORETICAL AND EXPERIMENTAL

The theoretical load-deflection relationship derived from the expressions in section 4 will not be the same as the load-deflection curve obtained in a test.

In figure 7.1 two examples of theoretical and experimental load-deflection relationships are shown.

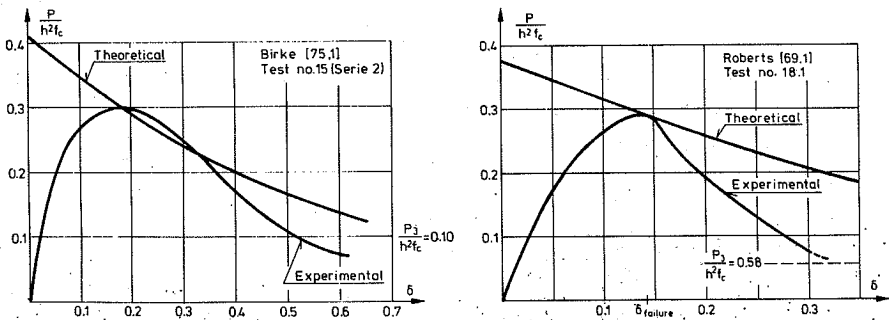


Figure 7.1: Theoretical and experimental load-deflection relationships. The theoretical curve is determined by using parameters derived from the tests and a value of  $\nu$  which approximately get the theoretical and experimental curves to intersect at the experimental maximum point.

As can be seen from the figure there is agreement between the theoretical and experimental curve in a small area only. This is partly caused by the descending branch of the stress-strain relationship for concrete in uniaxial compression after the maximum load is reached. This is also caused because the theoretical curve is determined by using the same assumption for all values of  $\delta$ , which is correct only for a small interval.

The same situation is also found in other cases, where the load bearing capacity is strongly influenced by the concrete strength. Examples of this are pure bending in an overly reinforced section and shear in beams.

#### 8. DESIGN RECOMMENDATIONS FOR ONE-WAY SLABS

The theoretical expressions from section 4 can be used, but they are complicated. As shown in section 5, the agreement obtained between test results and theory is found to be quite good, even if the theoretical expressions are modified. It appears from the analysis that the membrane action can be taken into account by adding a membrane moment,  $m_M$ , to the normal positive bending moment. The normal negative bending moment,  $m_J'$ , is unchanged. The moments are given by

$$m_J = \phi \left( \frac{d}{h} - \frac{\phi}{2\nu} \right) \cdot h^2 f_c \quad (8.1)$$

$$m_J' = \phi' \left( \frac{d}{h} - \frac{\phi'}{2\nu} \right) \cdot h^2 f_c \quad (8.2)$$

$$m_M = \frac{1}{4} h^2 \nu f_c \cdot (1 - \delta)^2 \quad (8.3)$$

where the effectiveness factor  $\nu$  and the relative deflection  $\delta$  can be determined by

$$\nu = \frac{4.39}{\sqrt{f_c}} \quad (f_c \text{ in MPa}) \quad (8.4)$$

$$\delta = \frac{\rho \lambda^2}{2\rho \lambda^2 + 4} + \delta_s, \quad \rho = 0.0035 \quad (8.5)$$



The constant 0.14 in the expression for the effectiveness factor (8.4) is, for reasons of simplicity, deleted here.

The calculations are carried out as a normal yield line calculation. The yield line pattern is determined for a one-way slab without membrane action. When the yield line pattern is fixed, the positive bending moment,  $m_J$ , is replaced by the sum of the positive bending moment and the membrane moment. The sum  $m_J + m_M$  is used instead of  $m_J$  in the otherwise normally used expressions for the load carrying capacity.

The relative deflection  $\delta_s$  in (8.5) can be determined according to the expressions in section 6.

## 9. CONCLUSION

In many cases the theory of plasticity gives a good description of the ultimate strength of concrete structures, in spite of the limited concrete ductility. Using a rigid plastic material model for concrete, modification factors must be used for taking into account the lack of ductility. The membrane action in reinforced concrete slab strips are dealt with by this model and encouraging results are obtained.

Expressions for the ultimate strength of reinforced concrete slab strips with horizontal restraints at the supports were derived. Comparison between the theoretical expressions and the test results gives good agreement. Since the expressions are too complicated for practical use, they were simplified. The modified expressions were also compared with test results and the agreement is quite good.

It turns out that the membrane action can be taken into account by adding a membrane moment to the normally used positive bending moment and considering the sum as the ultimate positive moment. The negative bending moment is unchanged. The calculations are then carried out as a normal yield line calculation.

10. REFERENCES

- [63.1] Christiansen, K.P.: The Effect of Membrane stresses on the ultimate strength of the interior panel in a reinforced concrete slab, *The Structural Engineer*, No. 8, Vol. 41, Aug. 1963, pp. 261-265.
- [68.1] Calladine, C.R.: Simple Ideas in the Large-Deflection Plastic Theory of Plates and Slabs, *Engineering Plasticity*, Heyman and Leckie, eds., Cambridge University Press, Cambridge, England, 1968, pp. 93-127.
- [69.1] Roberts, E.H.: Load-carrying Capacity of Slab Strips Restrained against Longitudinal Expansion, *Concrete*, Vol. 3, 1969, pp. 369-378.
- [75.1] Birke, Håkan: Kopoleffekt vid Betongplattor (Dome effect in concrete slabs), Report No. 108, Institutionen för Byggnadsstatik, Royal Technical University, Stockholm, Sweden, 1975.
- [80.1] Bræstrup, M.W. & Morley, C.T.: Dome Effect in RC Slabs: Elastic-Plastic Analysis, *Journal of the Structural Division*, ST 6, 15501, June 1980, pp. 1255-1262.
- [83.1] Christiansen, K.P. & Frederiksen, V.T.: Experimental investigation of rectangular concrete slabs with horizontal restraints, *Materials and Structures*, Vol. 16, No. 93, May-June 1983, pp. 179-192.
- [83.2] Christiansen, K.P. & Frederiksen, V.T.: Tests on rectangular concrete slabs with horizontal restraints on three sides only, *Institute of Building Design, Nordic Concrete Research*, 1983.
- [84.1] Nielsen, M.P.: Limit Analysis and Concrete Plasticity, Prentice-Hall, Inc., Englewood Cliffs, New Jersey, 1984.
- [85.1] Andreasen, B.S.: Trykmembranvirkning i betonplader (Compressive membrane action in concrete slabs), M.Sc. Thesis, Department of Structural Engineering, Technical University of Denmark, Lyngby, July 1985.

- [86.1] Andreassen, B.S. & Nielsen, M.P.: Dome Effect in Reinforced Concrete Slabs, Department of Structural Engineering, Technical University of Denmark, Rapport Serie R No. 212, 1986.
- [87.1] Yde, L.: Membrankræfter (Membrane forces), M.Sc. Thesis, Department of Structural Engineering, Technical University of Denmark, Lyngby, January 1987.
- [87.2] Nielsen, M.P. & Yde, L.: Bue- og kuppelvirkning i murværk (Arch and Dome Effect in Masonry), Nordisk Murværks-symposium, Copenhagen 1987.

AFDELINGEN FOR BÆRENDE KONSTRUKTIONER  
DANMARKS TEKNISKE HØJSKOLE

Department of Structural Engineering  
Technical University of Denmark, DK-2800 Lyngby

SERIE R

(Tidligere: Rapporter)

- R 249. NIELSEN, LEIF OTTO: Simplex Elementet. 1989.  
R 250. THOMSEN, BENDE DAHL: Undersøgelse af "shear lag" i det elasto-plastiske stadium. 1990.  
R 251. FEDDERSEN, BENT: Jernbetonbjælkens bæreevne. 1990.  
R 252. FEDDERSEN, BENT: Jernbetonbjælkens bæreevne, Appendix. 1990.  
R 253. AARKROG, PETER: A Computer Program for Servo Controlled Fatigue Testing Documentation and User Guide. 1990.  
R 254. HOLKMANN OLSEN, DAVID & NIELSEN, M.P.: Ny Teori til Bestemmelse af Revneafstande og Revnevidder i Betonkonstruktioner. 1990.  
R 255. YAMADA, KENTARO & AGERSKOV, HENNING: Fatigue Life Prediction of Welded Joints Using Fracture Mechanics. 1990.  
R 256. Resumeoversigt 1989 - Summaries of Papers 1989. 1990.  
R 257. HOLKMANN OLSEN, DAVID, GANWEI, CHEN, NIELSEN, M.P.: Plastic Shear Solutions of Prestressed Hollow Core Concrete Slabs. 1990.  
R 258. GANWEI, CHEN & NIELSEN, M.P.: Shear Strength of Beams of High Strength Concrete. 1990.  
R 259. GANWEI, CHEN, NIELSEN, M.P. NIELSEN, JANOS, K.: Ultimate Load Carrying Capacity of Unbonded Prestressed Reinforced Concrete Beams. 1990.  
R 260. GANWEI, CHEN, NIELSEN, M.P.: A Short Note on Plastic Shear Solutions of Reinforced Concrete Columns. 1990.  
R 261. GLUVER, HENRIK: One Step Markov Model for Extremes of Gaussian Processes. 1990.  
R 262. DAHL, KAARE, K.B.: Preliminary State-of-the-art Report on Multiaxial Strength of Concrete. 1990  
R 263. JØNSSON, JEPPE: Recursive Finite Elements for Buckling of Thin-walled Beams. 1990.  
R 264. NIELSEN, LEIF OTTO: FEM3 - prototype på problemgenerelt h-p FEM-program. 1990.  
R 265. PETERSEN, PETER, KRENK, STEEN og DAMKILDE, LARS: Stabilitet af rammer af tyndpladeprofiler. 1991.  
R 266. RIBERHOLT, HILMER og MORSING, NIELS: Limtræ af dansk træ, HQL-planker. 1991.  
R 267. ILIC, ALEKSANDAR: Konstruktionspatologi. 1991.  
R 268. Resumeoversigt 1990 - Summaries of Papers 1990. 1991.  
R 269. XIAOQING YIN: Constitutive Equations and their Application in finite Element Analysis. 1991.  
R 270. ARNBJERG-NIELSEN, TORBEN: Rigid-ideal plastic model as a reliability analysis tool for ductile structures. 1991.  
R 271. VILMANN, OLE: A Harmonic Half-Space Fundamental Solution. 1991.  
R 272. VILMANN, OLE: The Boundary Element Method applied in Mindlin Plate Bending Analysis. 1991.  
R 273. GANWAY, CHEN, ANDREASEN, B.S., NIELSEN, M.P.: Membrane Actions Tests of Reinforced Concrete Square Slabs. 1991.  
R 274. THOUGARD PEDERSEN, NIELS, AGERSKOV, H.: Fatigue Life Prediction of Offshore Steel Structures under Stochastic Loading. 1991.  
R 275. ANDREASEN, B.S., NIELSEN, M.P.: Arch Effect in Reinforced Concrete one-way Slabs. 1991.  
R 276. ASKEGAARD, VAGN: Prediction of Initial Crack Location in Welded Fatigue Test Specimens by the Thermoelastic Stress Analysis Technique. 1991.

...the ... of ...  
...the ... of ...  
...the ... of ...

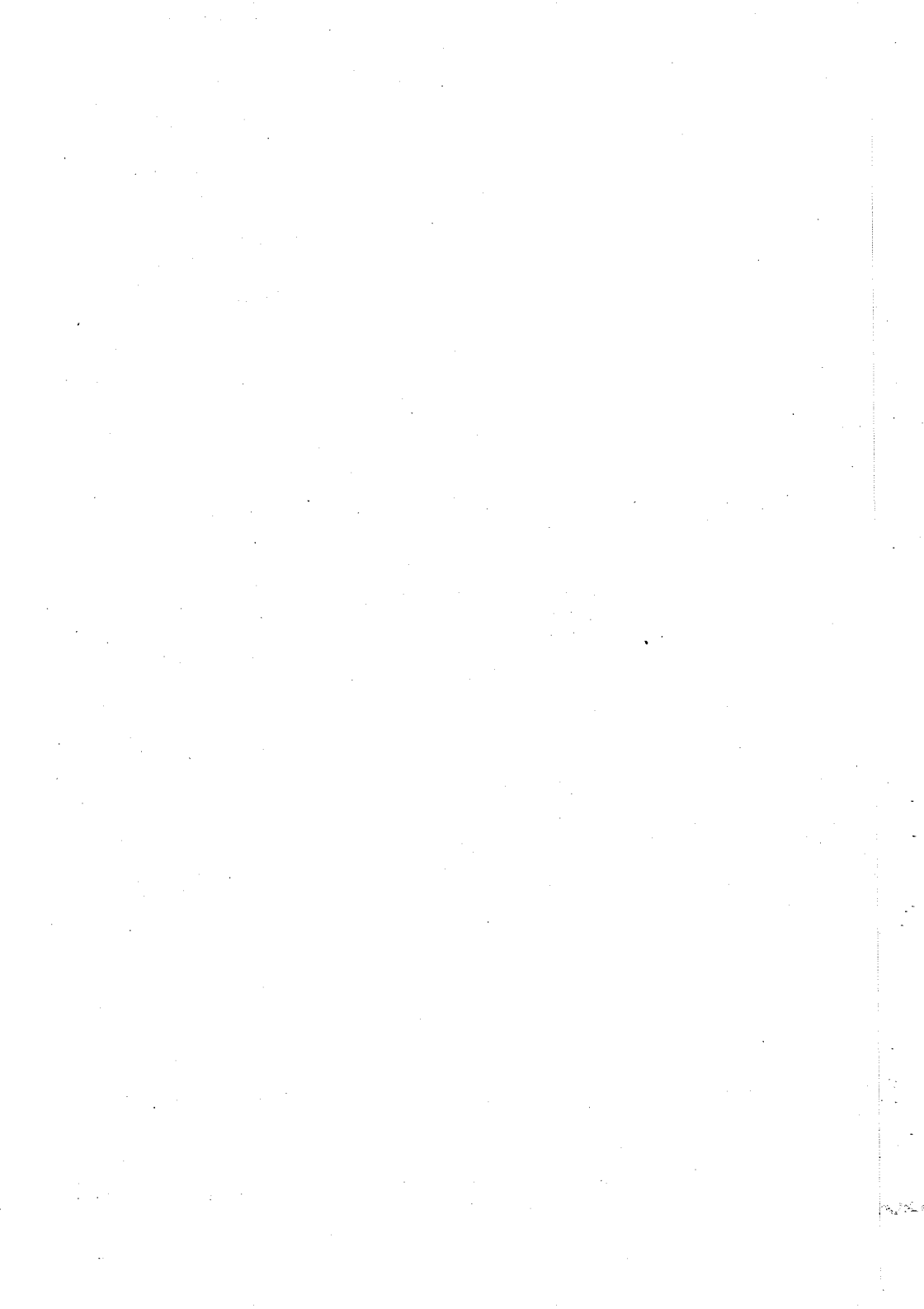
...the ... of ...  
...the ... of ...  
...the ... of ...

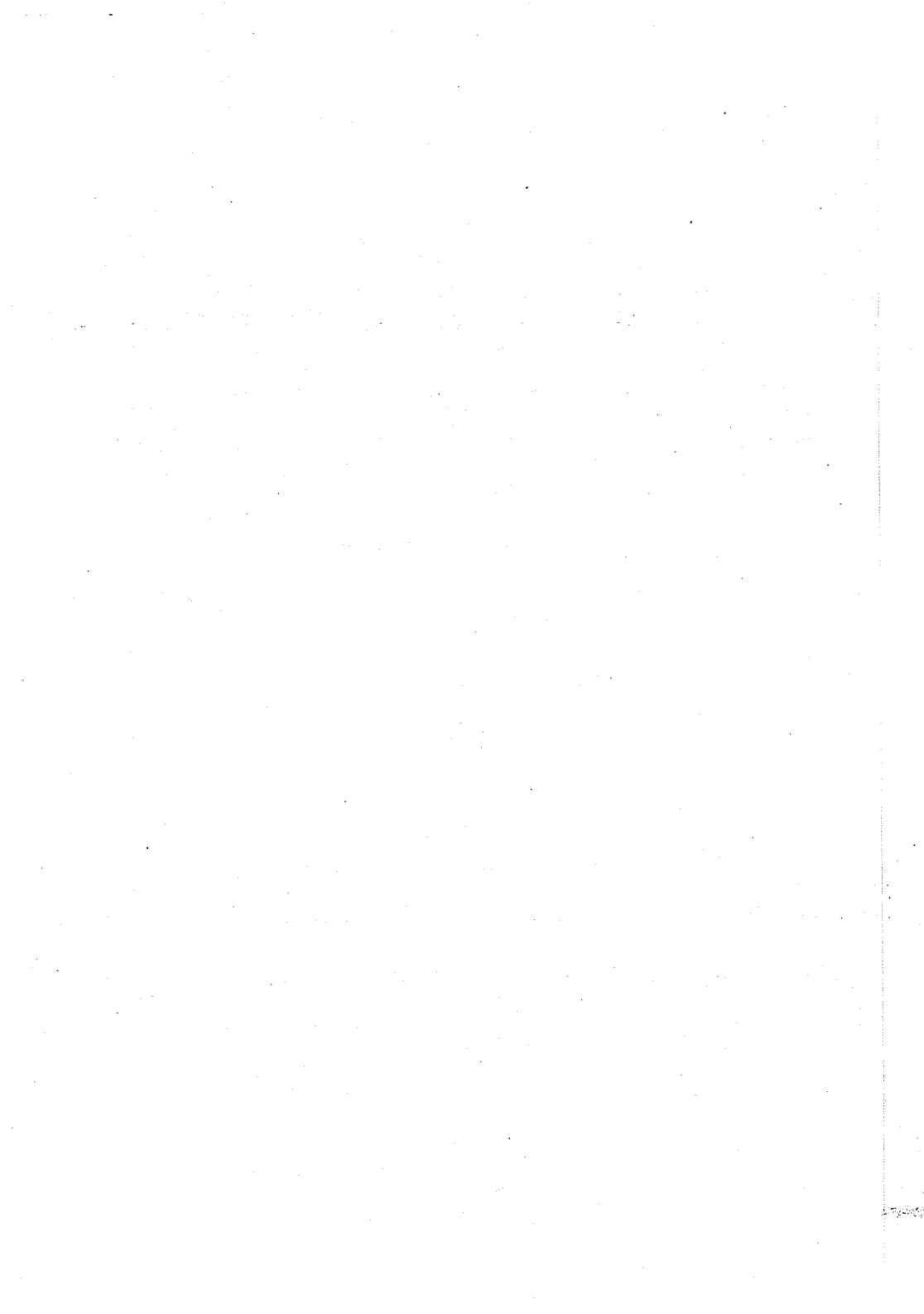
...the ... of ...  
...the ... of ...  
...the ... of ...

...the ... of ...  
...the ... of ...  
...the ... of ...

...the ... of ...  
...the ... of ...  
...the ... of ...

...the ... of ...  
...the ... of ...  
...the ... of ...





Hvis De ikke allerede modtager Afdelingens resumeoversigt ved udgivelsen, kan Afdelingen tilbyde at tilsende næste års resumeoversigt, når den udgives, dersom De udfylder og returnerer nedenstående kupon.

Returneres til  
Afdelingen for Bærende Konstruktioner  
Danmarks tekniske Højskole  
Bygning 118  
2800 Lyngby

Fremtidig tilsendelse af resumeoversigter udbedes af  
(bedes udfyldt med blokbogstaver):

Stilling og navn: .....

Adresse: .....

Postnr. og -distrikt: .....

The Department has pleasure in offering to send you a next year's list of summaries, free of charge. If you do not already receive it upon publication, kindly complete and return the coupon below.

To be returned to:  
Department of Structural Engineering  
Technical University of Denmark  
Building 118  
DK-2800 Lyngby, Denmark.

The undersigned wishes to receive the Department's  
List of Summaries:

(Please complete in block letters)

Title and name .....

Address.....

Postal No. and district.....

Country.....



The first step in the process of creating a new product is to identify a market need. This involves conducting market research to understand the current market landscape, customer preferences, and potential gaps in the market. Once a market need is identified, the next step is to develop a concept for the product that addresses this need.

Once a concept is developed, the next step is to create a prototype. This involves building a physical or digital model of the product to test its functionality and user experience. Prototyping allows designers to identify and address any issues or limitations before moving forward with full-scale production. This iterative process is crucial for ensuring the final product meets the needs of the target market.

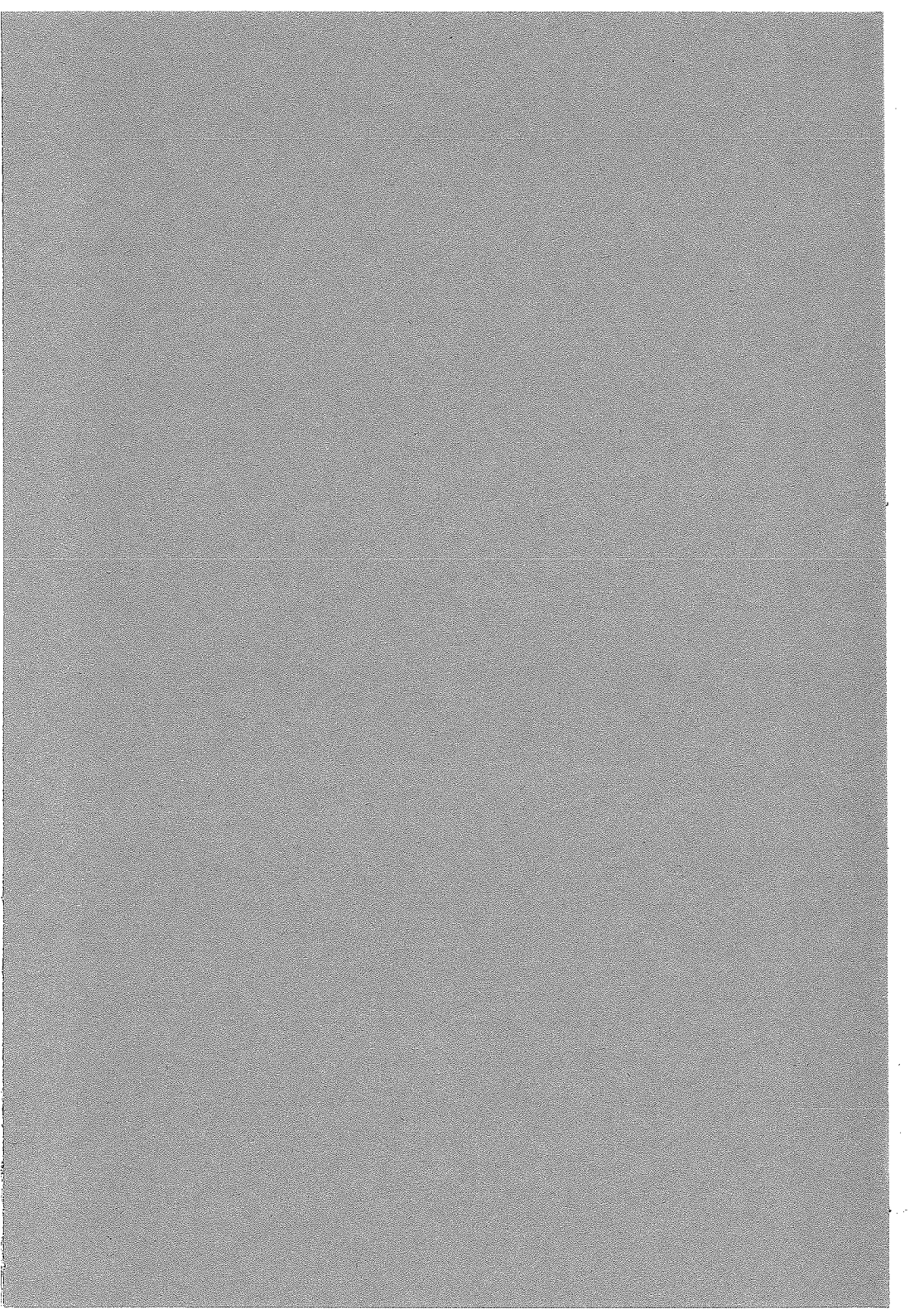
After the prototype is tested, the next step is to develop a detailed design and engineering plan. This includes creating technical drawings, specifications, and a bill of materials. The design team must also consider manufacturing processes and materials to ensure the product can be produced efficiently and at scale. This stage is critical for ensuring the product is both functional and cost-effective.

Once the design is finalized, the next step is to secure funding and resources for production. This may involve seeking investors, applying for grants, or using crowdfunding. The production phase involves manufacturing the product, which may include sourcing materials, setting up a production line, and quality control measures to ensure consistency and reliability.

After production, the final step is to launch the product into the market. This involves marketing and distribution strategies to reach the target audience. Marketing efforts may include social media campaigns, content marketing, and traditional advertising. Distribution channels should be carefully chosen to ensure the product is easily accessible to customers. Finally, the product should be monitored for performance and customer feedback to inform future improvements.

The product development process is a complex and iterative one that requires careful planning and execution. Each step is interconnected, and changes may be necessary throughout the process. By following these steps, businesses can increase their chances of creating a successful product that meets market needs and stands out in a competitive landscape.

Understanding the product development process is essential for any business looking to bring a new product to market. It involves a combination of creative thinking, technical expertise, and strategic planning. By staying organized and adaptable, businesses can navigate the challenges of product development and achieve their goals.



ISSN 0108-0768  
ISBN 87-7740-077-1

**ABC**

Serie R  
No 275